Apatinib Combined With Radiotherapy Enhances Antitumor Effects in an In Vivo Nasopharyngeal Carcinoma Model

Shanshan Liu, MD[1], Fei Wu, MD[2], Yanling Zhang, MD[3], Rongsheng Qin, MD[4], Nengping Zhu, MD[4], Yuan Li, MD[4], Mingting Wang, MD[4], Qin Zeng, MD[4], Danna Xie, MD[4], Yinghua Li, MD[4], Juan Fan, MD[4], and Yunwei Han, PhD[4]

Abstract

Vascular endothelial growth factor (VEGF) and its receptor (VEGFR) are highly expressed in nasopharyngeal carcinoma; therefore, blocking the binding of VEGF and VEGFR may be a potential way to treat nasopharyngeal carcinoma. Apatinib inhibits tumor angiogenesis. Previous studies have suggested that treatment with apatinib has an antitumor effect on nasopharyngeal carcinoma. This study will investigate the effect of apatinib combined with radiotherapy. In this study, nude mice injected with CNE-2 nasopharyngeal carcinoma cells were randomly divided into 6 groups. Therapeutic effects were assessed by evaluating tumor inhibition rate, phosphorylation of VEGFR-2, CD31, partial oxygen pressure, and tumor metabolism. We found that the tumor inhibition of mice in the treated groups was better compared to that of the control group. In mice treated with apatinib alone, angiogenesis was prevented, and the tumor tissue partial oxygen pressure was reduced, thereby achieving an antitumor effect. Moreover, the tumor inhibitory effect of combined treatment was stronger than treatment with either apatinib or radiotherapy alone. Compared with monotherapy treatment, combined treatment better resisted angiogenesis. Apatinib combined with radiotherapy to treat nasopharyngeal carcinoma has synergistic effects, which may be related to enhanced antiangiogenesis.

Keywords

apatinib, nasopharyngeal carcinoma, radiotherapy, angiogenesis, partial oxygen pressure

Received August 04, 2019. Received revised February 03, 2020. Accepted for publication March 31, 2020.

Introduction

Nasopharyngeal carcinoma (NPC) originated from of nasopharyngeal epithelium cells, and abnormal differences were found in race and geographical distribution. The highest incidence rate was found in southern China, southeast Asia, north Africa, and the Pacific islands.[1-4] Due to the anatomical position and radiosensitivity of NPC, radiotherapy remains the treatment of choice for NPC.[5] By continuously updating and advancing radiotherapy equipment and technology, the survival rate of NPC has been greatly improved. However, several patients are resistant to radiotherapy, which results in a reduction of the cure rate of NPC.[6] Therefore, reducing radiotherapy resistance may be the key target for improving the therapeutic effect of NPC.

[1] Department of General Medicine, The Affiliated Hospital of Southwest Medical University, Luzhou, China
[2] Department of Thyroid Surgery, The Affiliated Hospital of Southwest Medical University, Luzhou, China
[3] Department of Health Management, The Affiliated Hospital of Southwest Medical University, Luzhou, China
[4] Department of Oncology, The Affiliated Hospital of Southwest Medical University, Luzhou, China

Corresponding Authors:
Juan Fan and Yunwei Han, The Affiliated Hospital of Southwest Medical University, 25 Taiping Street, Luzhou, China.
Emails: fj-joan@163.com; 530018842@qq.com

The main function of radiotherapy is the disruption of double-stranded DNA, causing proteins to be blocked or initiate apoptosis to cause cell death.[7] Oxygen is an effective radioactive sensitizer, which can be released during the irradiation process to promote the production of reactive oxygen species/free radicals, resulting in major DNA damage.[8,9] As the tumor grows, the tumor microenvironment lacks sufficient blood supply, leading to low perfusion and hypoxia.[10] Clinical data have shown that hypoxia in tumor tissue associated with a poor treatment efficacy of many tumors including head and neck tumors.[11-13] Therefore, improving the blood supply and oxygen input of NPC tumor tissues may significantly improve the beneficial effect of radiotherapy in NPC.

Angiogenesis is a multistep process of new blood vessel formation involved in tumor development.[14,15] Angiogenic factors include vascular endothelial growth factor (VEGF), basic fibroblast growth factor, and insulin-like growth factor. Among them, vascular endothelial growth factor receptor-2 (VEGFR-2) is the main signal sensor of angiogenesis. During the stimulation of VEGF, VEGFR-2 is phosphorylated in the carboxyl terminal and kinase insertion area, thereby promoting angiogenesis.[16-19] In most patients with NPC, the VEGF/VEGFR complex was found to be overexpressed, which associated with an increased risk of metastasis of NPC and a reduction in survival time.[20-23]

Apatinib is a small molecule VEGFR-2 tyrosine kinase inhibitor that competes highly selectively for the Adenosine Triphosphate (ATP)-binding site of VEGFR-2, inhibits phosphorylation of VEGFR-2 (p-VEGFR2), and blocks VEGF and its receptor binding signaling transduction pathway. It strongly inhibits tumor angiogenesis and plays an antitumor role. Jain demonstrated that antiangiogenic drugs have a reshaped vascular system, which can result in blood vessel "normalization" of "time window."[24] In the "time window," antiangiogenic drugs briefly improve the function of the tumor vascular system, thereby increasing the interaction with oxygen, and reducing the pressure of the interstitial fluid. This has formed the theoretical basis for the combination of antiangiogenic drugs and radiotherapy. Teicher et al were the first to show that inhibiting angiogenesis enhances the therapeutic efficacy of radiotherapy treatment.[25] In addition, Peng et al demonstrated that apatinib decreased tumor microvascular density and increased cell apoptosis by inhibiting VEGFR-2, which had an antitumor effect on CNE-2 NPC.[26] Studies that report on the use of apatinib in combination with radiotherapy and its synergistic antitumor effects on NPC are limiting. The goal of this study was to explore the effect of apatinib combined with radiotherapy for the treatment of NPC and to provide guidance for future research and clinical practice.

Materials and Methods

Cell Lines and Mice

CNE-2 NPC cells were provided by the Experimental Center of the Affiliated Hospital of the Southwest Medical University (Luzhou, China), which were maintained in Roswell Park Memorial Institute (RPMI) medium at 37°C and 5% CO_2. Mycoplasma testing has been done for the cells used and no mycoplasma infection was found. Medium was replaced every 3 days.

BALB/c female nude mice (4-5 weeks of age, 18.85 ± 2.15 g) were purchased from Tengxin Biotechnology Co Ltd (Chongqing, China). Mice were housed in the animal research center of the Affiliated Hospital of Southwest Medical University. During the week prior to the experiment, animals were strictly kept in an air-clean laminar rack at a constant temperature ($24°C \pm 2°C$), constant humidity ($50\% \pm 10\%$ relative humidity), and specific pathogen-free environment. The mouse cage, air filter cover, bedding, food, and drinking water were sterilized and replaced in a sterile environment. Their care was in accordance with institution guidelines.

Drugs and Major Reagents

Apatinib was provided by Jiang Su Heng Rui Medicine Co Ltd (Jiangsu, China). Anti-CD31 monoclonal antibody was purchased from BioWorld Technology Co Ltd (Nanjing, China), and anti phosphorylation of VEGFR-2 (p-VEGFR-2) monoclonal antibody (Tyr951) was purchased from Cell Signaling Technology, Inc, Shanghai, China, and antibodies were affinity purified from rabbit antiserum and used at dilutions of 1:50 to 1:200.

Establishing and Experimental Design of the Tumor Model

Exponential phase CNE-2 cells were adjusted to 1×10^7 cells per 0.1 mL and injected into the right thigh of BALB/c nude mice. When the average volume of tumor reached 150 to 200 mm^3, mice were randomly divided into 6 groups (n = 8 per group) and received treatment as follows: (1) the control group was administered 0.1 mL normal saline (NS) per day on days 1 to 7, (2) the apatinib group received 200 mg/kg/d on days 1 to 7, (3) single radiotherapy 6 Gy group: 0.1 mL NS per day on days 1 to 7 and single radiotherapy (6 Gy) on day 8, (4) single radiotherapy 12 Gy group: 0.1 mL NS per day on days 1 to 7 and single radiotherapy (12 Gy) on day 8, (5) apatinib + 6 Gy: apatinib 200 mg/kg on days 1 to 7 and single radiotherapy (6 Gy) on day 8, (6) apatinib + 12 Gy: apatinib 200 mg/kg on days 1 to 7 and single radiotherapy (12 Gy) on day 8. The solvent for apatinib was NS, and both NS and apatinib were administered by gastric irrigation.

The tumor diameter (mm) along the major (a) and minor axes (b) were measured every 3 days using a Vernier caliper, and the volume (V; mm^3) of the tumor was calculated according to the Steel formula, $V = 0.5 \times a \times b^2$. At 18 days after the start of treatment, mice were euthanized by cervical dislocation, and the tumor growth inhibition rate was calculated as follows: (1 − average volume of experimental group/average volume of control group) × 100%. The combined effects of 2 types of treatments were determined by Q: Q = E(A + B) / [EA

+ (1 − EA) × EB], in which E (A + B) represented the inhibition rate of the combined group, whereas EA and EB represented the inhibitory rate of apatinib or radiotherapy, respectively. Q < 0.85 indicated that the 2 therapeutic effects were antagonistic to each other, 0.85 < Q < 1.15 indicated an additive effect of these 2 therapeutic effects, while Q > 1.15 indicated a synergistic effect of the 2 therapeutic treatments.

Radiation Approach

Nude mice were installed in a homemade Plexiglas box, and the hind limbs containing the tumor were pulled out and fixed with a string. The tumor site was exposed to the center of the field and was located more than 1 cm from the edge of the field. The upper and lower parts of the irradiation were filled with 2-cm oil yarn, the remainder of the mouse's body was outside the field.

Micro 18F-FDG Positron Emission Tomography/Computed Tomography Imaging

One day after treatment, mice were anesthetized by 1% pentobarbital sodium. After the tail vein injection with contrast agent (18F-FDG)150 to 200 uCi, the positron emission tomography/computed tomography (PET/CT) (Siemens, Inveon, Berlin, Germany) was performed using a 20-minute scan. After applying correction factors, an image representing the 18F-FDG distribution was obtained. The region of interest (ROI) covering the entire tumor was drawn manually. In addition, ROIs were drawn on the contralateral paraspinal muscles. The standard uptake value (SUV) in the tumor site and in contralateral paraspinal muscles was determined. The ratio of the maximum SUV of the tumor and the maximum SUV to the contralateral paraspinal muscles represented the T/M (the ratio of the maximum SUV of the tumor and the maximum SUV to the contralateral paraspinal muscles) value.

Unisense-Dissolved Oxygen Microelectrode to Detect Tumor Tissue Partial Oxygen Pressure

A Unisense-dissolved oxygen microelectrode is a miniaturized Clark-type dissolved oxygen microelectrode with a protective cathode. In this study, after the mice were euthanized, the tumor tissue was immediately removed and the tumor long axis and short axis were measured. Each tumor was measured in 4 parts, including 1/16 short axis, 1/8 short axis, 1/4 short axis, and 1/2 short axis. After the average value of each part was measured, the average of the partial oxygen pressure of the 4 parts was considered the partial oxygen pressure of the tumor tissue. The total time for each mouse from death to test was less than 5 minutes.

Phosphorylation of VEGFR-2 and CD31 Immunohistochemical Detection in Tumor Specimens

Prior to embedding in paraffin, tumor tissue was fixed in 10% formalin solution. All experiments were strictly carried out according to the manufacturer's guidelines. Microscopic evaluation was performed at ×400 magnification and showed that the cell membrane or cytoplasm appeared as a brownish-yellow or brown color, indicating p-VEGFR-2 expression in the membrane or cytoplasm. From each section, a total of 5 views were randomly selected, and the percentage of positive cells per field cells was counted. The average of the 5 percentages was considered the percentage of p-VEGFR-2-positive cells in the section.

The microvessel density (MVD) was quantified according to the method described by Weidner et al.[27] First, screening was performed at a low magnification (×100) to scan the tumor area and to identify the most intensive areas of vascularization, designated as "hot spots." In these hot spots, the microvessels were counted using a high-power magnification field (×400). The MVD was expressed as the number of microvessels per field. Endothelial cells, identified by CD31 staining, that were clearly separated from adjacent microvessels, tumor cells or connective tissue were considered microvessels. In each section, 5 hot spots were selected for microvascular counts, the average represented the MVD of the section.

Statistical Analyses

Data analyses were performed using SPSS software version 17.0 (SPSS, Inc, Chicago, Illinois). Data were expressed as the mean ± standard deviation. Comparisons between multiple groups were made using the 1-way analysis of variance test. P < .05 was considered statistically significant.

Results

Antitumor Effect of Apatinib Combined With Radiotherapy

When the average volume of tumor reached 150 to 200 mm3 and treated with various treatments. Figure 1 presents the average volume of tumor xenografts per group from 1 to 18 days posttreatment, and the statistical analysis was performed including all groups. In the control group, the tumor growth was increased compared to the other groups (P < .05). The inhibition effect of 12 Gy group better than that of 6 Gy group (P < .05). In addition, there was no difference between the 6 Gy group and the apatinib group (P > .05). Moreover, the inhibition of tumor growth in mice in the apatinib + radiotherapy combination group was stronger compared to apatinib treatment or radiotherapy treatment alone (P < .05).

Table 1 presents the tumor volume and inhibition rate per treatment group. The tumor inhibition rate of apatinib, 6 Gy alone, 12 Gy alone, apatinib + 6 Gy, and apatinib + 12 Gy were 33.3%, 38.8%, 61.5%, 63.8%, and 85.9%, respectively. Thus, the inhibition rate of apatinib + radiotherapy was higher compared to that of apatinib or radiotherapy group alone (P < .05). The Q value of apatinib + 6 Gy was 1.079 (Q value was
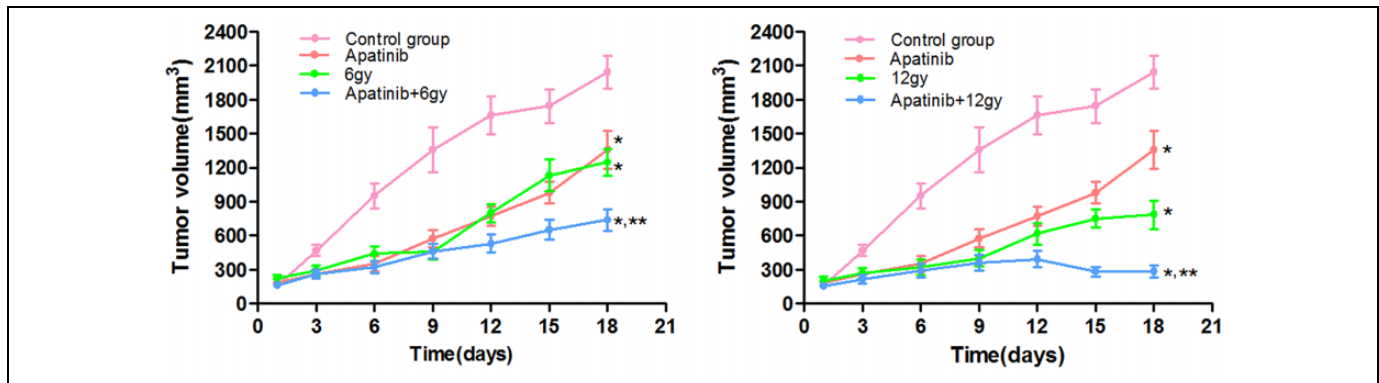
Figure 1. Tumor growth curve. Average volume of tumors xenograft into nude mice from 1 to 18 days' post treatment, and the statistical analysis was performed including all groups; *P < .05 versus the control group, **P < .05 versus the individual treatment group.

Table 1. Tumor Inhibition Rate.[a]

Groups	N	Tumor Volume(mm^3)	Tumor Inhibition Rate (%)
Control group	8	2042 ± 143.12233	
Apatinib	8	1360 ± 166.28289[b]	33.3
6 Gy	8	1248 ± 118.09530[b]	38.8
12 Gy	8	785 ± 125.19984[b]	61.5
Apatinib + 6 Gy	8	738 ± 92.44458[b,c]	63.8
Apatinib + 12 Gy	8	286 ± 52.28767[b,d]	85.9

[a]The tumor volume and inhibition rate determined on the 18th day.
[b]P < .05 versus the control group.
[c]P < .05 versus the apatinib group, 6 Gy.
[d]P < .05 versus the apatinib group, 12 Gy.

0.85-1.15), indicating that the therapeutic effect of apatinib + 6 Gy included the addition of the 2 individual treatments. The Q value of apatinib + 12 Gy was 1.156 (Q value >1.15), indicating that the therapeutic effect of apatinib + 12 Gy had a synergistic effect when compared with the treatment effect of individual treatment. Because the 2 combined treatment groups showed a Q value of >0.85, it was suggested that apatinib treatment combined with radiotherapy had a synergistic effect on the treatment of NPC.

Micro 18F-FDG PET/CT Imaging

Positron emission tomography/CT examination was performed the day after the treatment regimen was completed, and the results of PET/CT imaging on the transplantation of NPC in nude mice are shown in Figure 2. The tumor metabolism of control mice was significantly higher compared to that of treated mice (P < .05). Moreover, the tumor metabolism of 12 Gy–treated mice was lower compared to that of the 6 Gy–treated mice (P < .05). Mice treated with a combination of apatinib and radiotherapy showed a lower tumor metabolism compared to mice treated with apatinib or radiotherapy alone (P < .05). Therefore, we concluded that apatinib combined with radiotherapy had a synergistic inhibitory effect on the tumor metabolism in NPC.

Tumor Tissue Partial Oxygen Pressure Condition

After different treatment regimens and completion of PET/CT examination, the partial oxygen pressure of tumor tissues was determined. Figure 3 shows the results of the partial oxygen pressure of tumor tissues per treatment group. The tumor partial oxygen pressure in the control group was significantly higher compared to that of the other groups (P < .05). Moreover, the partial oxygen pressure of tumor tissue in 12 Gy–treated mice was lower compared to that of 6 Gy–treated mice (P < .05). The tumor partial oxygen pressure in the combined group was lower compared to that in mice that were treated with apatinib or radiotherapy alone (P < .05).

Immunohistochemistry Using Antibodies Directed Against p-VEGFR-2 and CD31

Immunohistochemical staining of xenografts using an antibody directed against p-VEGFR-2 revealed the effects of different treatment regimens and showed that the proportion of p-VEGFR-2 positive cells in each treatment group was different (Figure 4). The highest proportion of positive cells was observed in the control group (P < .05). The proportion of p-VEGFR-2 positive cells in 12 Gy–treated mice was lower compared to that in 6 Gy–treated mice (P < .05). Moreover, the proportion of p-VEGFR-2 positive cells in mice in the combined treatment group was lower compared to that in mice that were treated with either apatinib or radiotherapy alone (P < .05).

CD31-positive cells had a brownish appearance and showed a heterogeneous distribution in tumor tissues (Figure 5) and was used for the determination of MVD, which was used as a marker of angiogenesis. The MVD of mice in the control group was higher compared to that of mice in other groups (P < .05). The MVD in 12 Gy–treated mice was lower compared to that of 6 Gy–treated mice (P < .05). Moreover, the MVD of mice that were treated with a combination of apatinib + radiotherapy was lower compared to mice that were treated with apatinib or radiotherapy alone (P < .05).
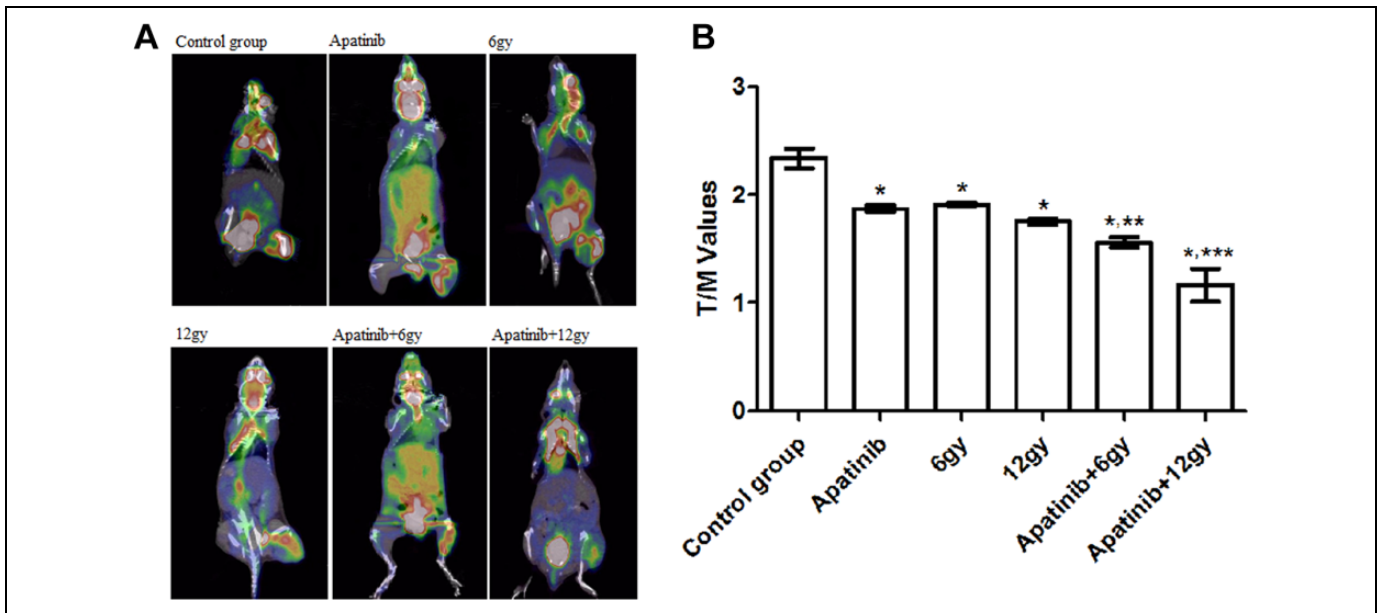
Figure 2. Micro 18F-fluorodeoxyglucose (FDG) positron emission tomography/computed tomography (PET/CT) imaging. A, Representative 18F-FDG PET scans of mice one day posttreatment with various regimens. B, T/M (the ratio of the maximum SUV of the tumor and the maximum SUV to the contralateral paraspinal muscles) associated with various treatment regimens. *P < .05 versus the control group. **P < .05 versus the apatinib group, 6 Gy. ***P < .05 versus the apatinib group, 12 Gy.
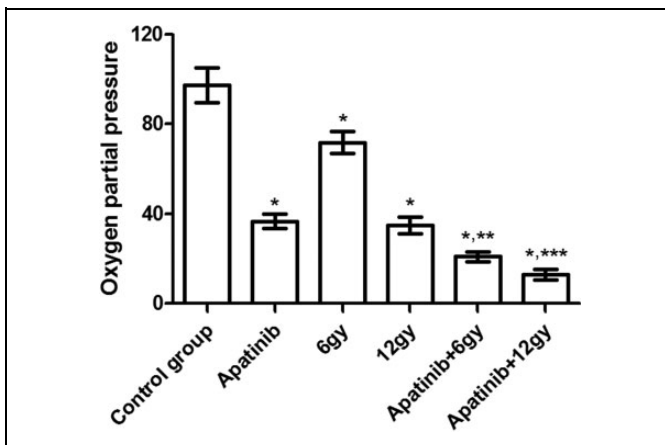
Figure 3. Tumor tissue partial oxygen pressure. Partial oxygen pressure was determined after the mice were euthanized. *P < .05 versus the control group. **P < .05 versus the apatinib group, 6 Gy. ***P < .05 versus the apatinib group, 12 Gy.

Discussion

Apatinib is a small molecular VEGFR-2 tyrosine kinase inhibitor, which can inhibit tumor angiogenesis and thereby achieve an antitumor effect. Many studies have shown that VEGF/VEGFR overexpression is observed in patients with NPC. Peng et al showed that apatinib has an antitumor effect on CNE-2 NPC and has a synergistic effect with cisplatin by inhibiting VEGFR-2.[26] In this study, we explored the effects of apatinib combined with radiotherapy for treating NPC in a mouse xenograft model.

Our study showed that apatinib had antitumor effects. By gradually increasing the radiation dose, the tumor growth of mice that underwent radiation alone gradually increased. In mice treated with a combination of apatinib and radiotherapy, tumor growth was significantly inhibited, and the inhibitory effect was higher compared to the effect of treatment with apatinib or radiotherapy alone. The combined effect Q showed that apatinib was synergistic with the combination of radiotherapy in the treatment of NPC.

The VEGF/VEGFR-2 signaling pathway is the main pathway involved in angiogenesis. Apatinib inhibits angiogenesis through inhibiting p-VEGFR-2 and reduces nutrition and oxygen supply of tumor tissue. Compared with mice in the individual treatment groups, mice in the combined treatment groups showed better inhibition of the expression of p-VEGFR-2 in the tumor, inhibition of angiogenesis, and reduction in the nutrition and oxygen supply of tumor tissue. We hypothesized that apatinib may be able to briefly improve the hypoxia state of the tumor, however due to the strong inhibition of angiogenesis and the reduction in oxygen supply, the measured partial oxygen pressure decreased. The antiangiogenic effect of the combination treatment was stronger compared to the effect of apatinib treatment alone, resulting in a lower partial oxygen pressure in the tumor. Antibodies directed against VEGFR-2 (DC101) combined with radiotherapy inhibited tumor angiogenesis and thereby showed a synergistic antitumor effect. The degree of hypoxia in mice that received combination treatment was significantly higher compared to mice that received monotherapy treatment.[28] Treatment with cediranib (AZD2171) combined with radiotherapy increased the
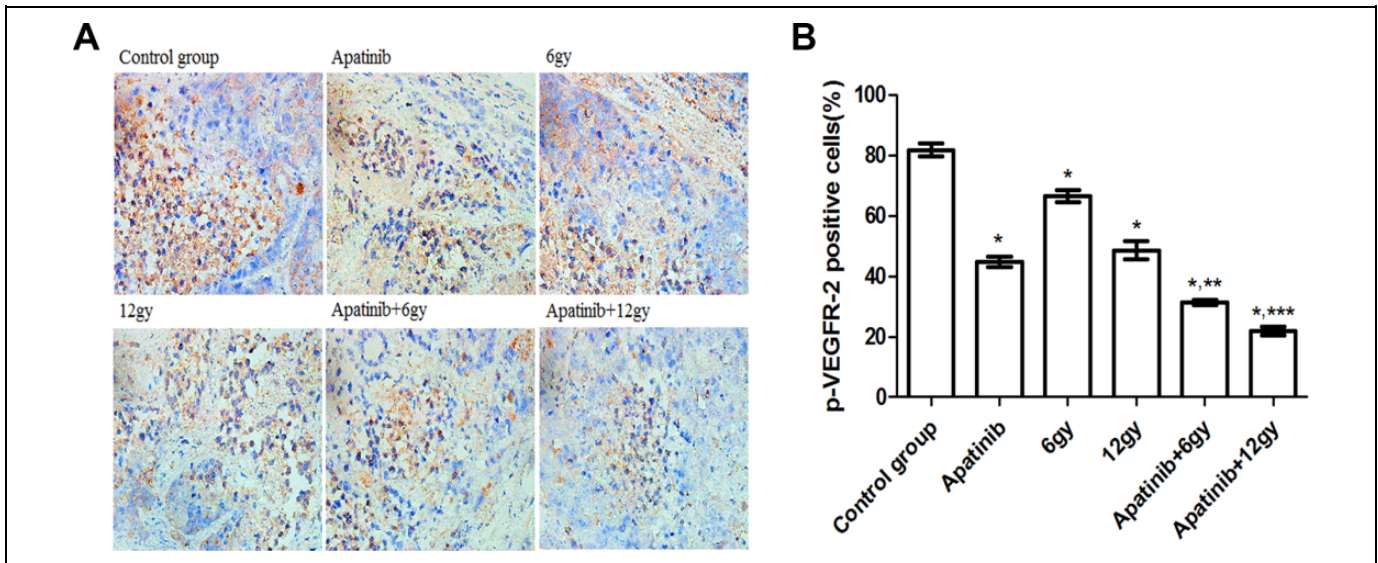
Figure 4. Expression of phosphorylation of VEGFR-2 (p-VEGFR-2) in CNE-2 nasopharyngeal carcinoma (NPC) tumor tissue. A, Immunohistochemical staining of xenograft CNE-2 NPC mice treated with various treatment regimens with a p-VEGFR-2 antibody. B, p-VEGFR-2 positivity (%) within treatment groups. *$P < .05$ versus the control group. **$P < .05$ versus the apatinib group, 6 Gy. ***$P < .05$ versus the apatinib group, 12 Gy.
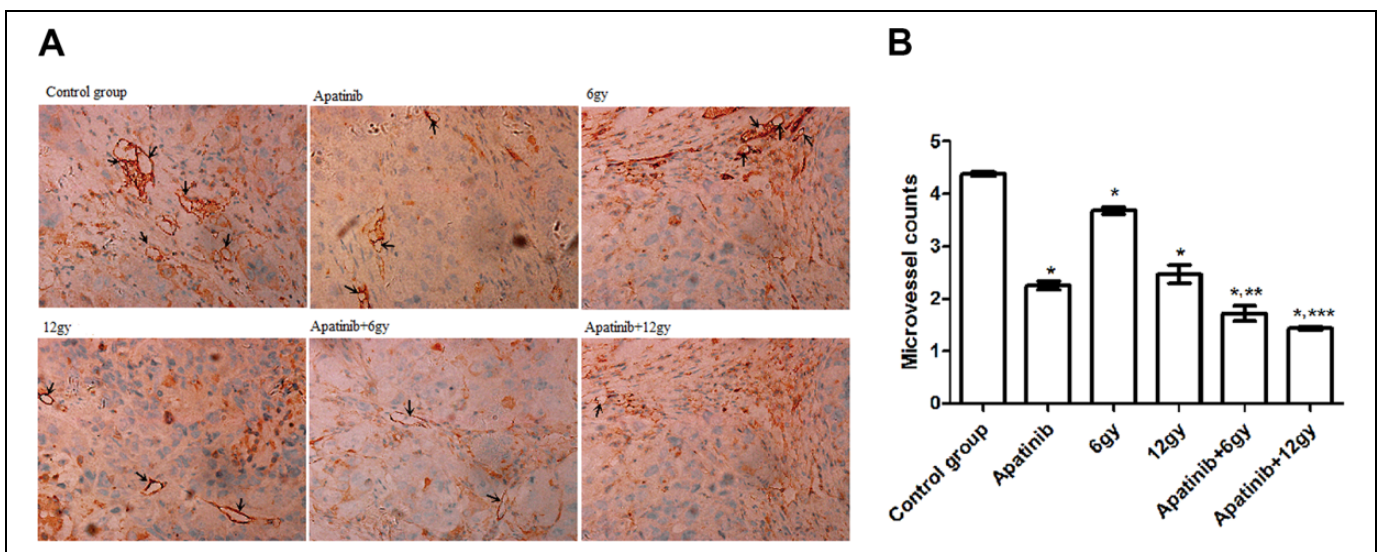

Figure 5. Expression of CD31 in CNE-2 nasopharyngeal carcinoma (NPC) tumor tissue. A, Immunohistochemical staining of xenograft mice treated with various treatment regimens using a CD31 antibody revealed the differences in microvessel density. B, Histograms showing the number of vessels in each group. *$P < .05$ versus the control group. **$P < .05$ versus the apatinib group, 6 Gy. ***$P < .05$ versus the apatinib group, 12 Gy.

degree of hypoxia in tumor tissue.[29] These findings were consistent with the results of our study. We found that, compared with the apatinib + 6 Gy–treated mice ($Q = 1.079$), apatinib + 12 Gy–treated mice ($Q = 1.156$) showed a better antitumor effect. Moreover, the results indicated that the main mechanism of synergistic inhibition of apatinib and radiotherapy in NPC treatment may involve the inhibition of angiogenesis.

The metabolism of tumor cells is vigorous. As the most widely used metabolic imaging agent, 18F-FDG can

quantitatively analyze the glucose metabolism of tumor. The PET-CT examination is widely used for the evaluation of tumor metabolism. Tumors with poor fluorodeoxyglucose (FDG) uptake tend to respond more favorably to treatment, whereas tumors that rapidly uptake FDG tend to respond poorly to treatment and have a worse prognosis.[26] The ratio of the maximum SUV of the tumor and the maximum SUV to the contralateral paraspinal muscles represented the T/M value. The higher the FDG uptake in tumor tissues, the higher the

T/M value, and vice versa. Groves et al showed that 18F-FDG uptake was highly significantly associated with angiogenesis in early breast cancer, and 18F-FDG PET might have a role in the management of patients with primary breast cancer even in early stage disease.[30] Kaira et al showed that the amount of 18F-FDG uptake in metastatic pulmonary tumors was determined by the presence of glucose metabolism (Glut1), phosphorylation of glucose (hexokinase I), hypoxia (HIF-1a), and angiogenesis (VEGF and MVD).[31] Guo et al showed that angiogenesis correlated positively with 18F-FDG uptake in lung adenocarcinomas.[32] Kaira et al showed that the metabolic activity of primary tumors as evaluated by PET study with 18F-FMT and 18F-FDG was related to tumor angiogenesis and the proliferative activity in non-small cell lung cancer.[33] Studies had also shown that 18F-FDG kinetics were modulated by angiogenesis-related gene.[34] The above studies found a positive correlation between tumor FDG uptake and angiogenesis. In this study, we hypothesized that reduced FDG uptake in the treatment group may also be associated with reduced angiogenesis, and the combined treatment group reduced tumor metabolism by inhibiting angiogenesis, thus achieving synergistic antitumor effect.

In summary, apatinib has antitumor effects on NPC, and there was a synergistic effect of apatinib combined with radiotherapy for NPC. Compared with the apatinib + 6 Gy–treated mice, apatinib + 12 Gy–treated mice showed a better antitumor effect. According to the data presented above, the following hypotheses were proposed: (1) Apatinib inhibited tumor angiogenesis by inhibiting p-VEGFR-2, reduced MVD, and reduced tissue partial oxygen pressure to achieve antitumor effects; (2) Apatinib combined with radiotherapy enhanced antiangiogenesis, thereby enhancing antitumor effects; (3) The main mechanism of the synergistic antitumor effects of apatinib and radiotherapy involves enhancing antiangiogenesis.

Authors' Note

Acknowledgments

Declaration of Conflicting Interests

Funding

ORCID iD

Yunwei Han https://orcid.org/0000-0002-6694-5846

References

1. Torre LA, Bray F, Siegel RL, Ferlay J, Lortet-Tieulent J, Jemal A. Global cancer statistics, 2012. *CA Cancer J Clin*. 2015;65(2): 87-108. doi:10.3322/caac.21262.

2. Chen W, Zheng R, Baade PD, et al. Cancer statistics in China, 2015. *CA Cancer J Clin*. 2016;66(2):115-132. doi:10.3322/caac. 21338.

3. Chua MLK, Wee JTS, Hui EP, et al. Nasopharyngeal carcinoma. *Lancet*. 2016;387(10022):1012-1024. doi:10.1016/S0140-6736(15)00055-0.

4. Cao SM, Simons MJ, Qian CN. The prevalence and prevention of nasopharyngeal carcinoma in China. *Chin J Cancer*. 2011;30(2): 114-119.

5. Sun Y, Li WF, Chen NY, et al. Induction chemotherapy plus concurrent chemoradiotherapy versus concurrent chemoradiotherapy alone in locoregionally advanced nasopharyngeal carcinoma: a phase 3, multicentre, randomised controlled trial. *Lancet Oncol*. 2016;17(11):1509-1520. doi:10.1016/S1470-2045(16)30410-7.

6. DeNittis AS, Liu L, Rosenthal DI, Machtay M. Nasopharyngeal carcinoma treated with external radiotherapy, brachytherapy, and concurrent/ adjuvant chemotherapy. *Am J Clin Oncol*. 2002; 25(1):93-95.

7. Zhou BB, Elledge SJ. The DNA damage response: putting checkpoints in perspective. *Nature*. 2000;408(6811):433-439. doi:10. 1038/35044005.

8. Karar J, Maity A. Modulating the tumor microenvironment to increase radiation responsiveness. *Cancer Biol Ther*. 2009; 8(21):1994-2001. doi:10.4161/cbt.8.21.9988.

9. Koch CJ, Kruuv J, Frey HE. Variation in radiation response of mammalian cells as a function of oxygen tension. *Radiat Res*. 1973;53(1):33-42.

10. Yeom CJ, Zeng L, Zhu Y, Hiraoka M, Harada H. Strategies to assess hypoxic/HIF-1-active cancer cells for the development of innovative radiation therapy. *Cancers*. 2011;3(3):3610-3631. doi:10.3390/cancers3033610.

11. Vaupel P. Prognostic potential of the pre-therapeutic tumor oxygenation status. *Adv Exp Med Biol*. 2009;645:241-246. doi:10.1007/978-0-387-85998-936.

12. Brizel DM, Sibley GS, Prosnitz LR, Scher RL, Dewhirst MW. Tumor hypoxia adversely affects the prognosis of carcinoma of the head and neck. *Int J Radiat Oncol Biol Phys*. 1997;38(2): 285-289. doi:10.1016/s0360-3016(97)00101-6.

13. Brizel DM, Scully SP, Harrelson JM, et al. Tumor oxygenation predicts for the likelihood of distant metastases in human soft tissue sarcoma. *Cancer Res*. 1996;56(5):941-943.

14. Hicklin DJ, Ellis LM. Role of the vascular endothelial growth factor pathway in tumor growth and angiogenesis. *J Clin Oncol*. 2005;23(5):1011-1027. doi:10.1200/JCO.2005.06.081.

15. Folkman J. Angiogenesis: an organizing principle for drug discovery? *Nat Rev Drug Discov*. 2007;6(4):273-286. doi:10.1038/nrd2115.

16. Shibuya M. VEGFR and type-V RTK activation and signaling. *Cold Spring Harbor Perspect Boil*. 2013;5(10):a009092. doi:10.1101/cshperspect.a009092.

17. Glade-Bender J, Kandel JJ, Yamashiro DJ. VEGF blocking therapy in the treatment of cancer. *Expert Opin Biol Ther*. 2003;3(2):263-276. doi:10.1517/14712598.3.2.263.

18. Tian S, Quan H, Xie C, et al. YN968D1 is a novel and selective inhibitor of vascular endothelial growth factor receptor-2 tyrosine kinase with potent activity in vitro and in vivo. *Cancer Sci*. 2011;102(7):1374-1380. doi:10.1111/j.1349-7006.2011.01939.x.

19. Holmes K, Roberts OL, Thomas AM, Cross MJ. Vascular endothelial growth factor receptor-2: structure, function, intracellular signalling and therapeutic inhibition. *Cell Signal*. 2007;19(10):2003-2012. doi:10.1016/j.cellsig.2007.05.013.

20. Guang-Wu H, Sunagawa M, Jie-En L, et al. The relationship between microvessel density, the expression of vascular endothelial growth factor (VEGF), and the extension of nasopharyngeal carcinoma. *Laryngoscope*. 2000;110(12):2066-2069. doi:10.1097/00005537-200012000-00017.

21. Hui EP, Chan AT, Pezzella F, et al. Coexpression of hypoxia-inducible factors 1alpha and 2alpha, carbonic anhydrase IX, and vascular endothelial growth factor in nasopharyngeal carcinoma and relationship to survival. *Clin Cancer Res*. 2002;8(8):2595-2604.

22. Li YH, Hu CF, Shao Q, et al. Elevated expressions of survivin and VEGF protein are strong independent predictors of survival in advanced nasopharyngeal carcinoma. *J Transl Med*. 2008;6:1. doi:10.1186/1479-5876-6-1.

23. Sha D, He YJ. Expression and clinical significance of VEGF and its receptors Flt-1 and KDR in nasopharyngeal carcinoma [in Chinese]. *Ai Zheng*. 2006;25(2):229-234.

24. Jain RK. Normalization of tumor vasculature: an emerging concept in antiangiogenic therapy. *Science*. 2005;307(5706):58-62. doi:10.1126/science.1104819.

25. Teicher BA, Holden SA, Ara G, et al. Influence of all anti-angiogenic treatment on 9L gliosarcoma, oxygenation and response to cytotoxic therapy. *Int J Cancer*. 1995;61(5):732-773. doi:10.1002/ijc.2910610523.

26. Peng QX, Han YW, Zhang YL, et al. Apatinib inhibits VEGFR-2 and angiogenesis in an in vivo murine model of nasopharyngeal carcinoma. *Oncotarget*. 2017;8(32):52813-52822.

27. Weidner N, Semple JP, Welch WR, Folkman J. Tumor angiogenesis and metastasis—correlation in invasive breast carcinoma. *N Engl J Med*. 1991;324(1):1-8. doi:10.1056/NEJM199101033240101.

28. Fenton BM, Paoni SF, Ding I. Pathophysiological effects of vascular endothelial growth factor receptor-2-blocking antibody plus fractionated radiotherapy on murine mammary tumors. *Cancer Res*. 2004;64(16):5712-5719. doi:10.1158/0008-5472.CAN-04-0434.

29. Williams KJ, Telfer BA, Shannon AM, Babur M, Stratford IJ, Wedge SR. Combining radiotherapy with AZD2171, a potent inhibitor of vascular endothelial growth factor signaling: pathophysiologic effects and therapeutic benefit. *Mol Cancer Ther*. 2007;6(2):599-606. doi:10.1158/1535-7163.MCT-06-0508.

30. Groves AM, Shastry M, Rodriguez-Justo M, et al. 18F-FDG PET and biomarkers for tumour angiogenesis in early breast cancer. *Eur J Nucl Med Mol Imaging*. 2011;38(1):46-52. doi:10.1007/s00259-010-1590-2.

31. Kaira K, Okumura T, Ohde Y, et al. Correlation between 18F-FDG uptake on PET and molecular biology in metastatic pulmonary tumors. *J Nucl Med*. 2011;52(5):705-711. doi:10.2967/jnumed.111.087676.

32. Guo J, Higashi K, Ueda Y, et al. Microvessel density: correlation with 18F-FDG uptake and prognostic impact in lung adenocarcinomas. *J Nucl Med*. 2006;47(3):419-425.

33. Kaira K, Oriuchi N, Shimizu K, et al. Correlation of angiogenesis with 18F-FMT and 18F-FDG uptake in non-small cell lung cancer. *Cancer Sci*. 2009;100(4):753-758. doi:10.1111/j.1349-7006.2008.01077.x.

34. Strauss LG, Koczan D, Klippel S, et al. Impact of angiogenesis-related gene expression on the tracer kinetics of 18F-FDG in colorectal tumors. *J Nucl Med*. 2008;49(8):1238-1244. doi:10.2967/jnumed.108.051599.